

# Current Saturation in Nonmetallic Field Emitters

Stanislav S. Baturin

*PSD Enrico Fermi Institute, The University of Chicago,  
5640 S. Ellis Ave., Chicago, IL 60637, USA\**

Alexander V. Zinovev

*Materials Science Division, Argonne National Laboratory,  
9700 S. Cass Ave., Argonne, IL 60439, USA*

Sergey V. Baryshev

*Department of Electrical and Computer Engineering,  
Michigan State University, 428 S. Shaw Ln., East Lansing, MI 48824, USA†*

Field emission from metals was well understood nearly a century ago. Description of its core process given by Fowler and Nordheim was an early success of emerging quantum mechanics. It paved the way to field emission and ion microscopy that were the first methods that imaged metal surfaces at nanometer and atomic resolution. Contrastively, in 1960's and later on it was discovered that nonmetallic (III-V and II-VI semiconductors, diamond, carbon nanotubes, amorphous carbon) field emitters do not obey the very basic Fowler-Nordheim law. In experiments, the output current stops growing with the electric field, and current-voltage characteristic switches from diode-like to resistor-like behavior. This general phenomenon, present in such a broad spectrum of materials, is referred to as current saturation effect and has remained unexplained for more than five decades. Here, we propose a unified and transparent concept that explains the current saturation effect in any nonmetallic field emitter.

**Introduction** Field emission electron sources are the basis for cutting-edge microscopy [1, 2], X-ray medical devices [3], mass spectrometers [4], high power systems [5–9], satellite thrusters (see [10] and references therein) and many other applications. In the realm of finding inexpensive and reliable field emission devices, beyond Spindt cathodes [11, 12], that can simplify and scale complex systems packaging via thin film and micro- and nano-fabrication technologies, many novel advanced materials are studied. Main emphasis is being placed on exploring new field emission materials [13–15] or engineering traditional semiconductor materials [3, 16, 17], or both [18]. In other words, advanced device fabrication technologies are focused on materials that are not traditional metals. These nonmetallic materials often have very low turn-on fields that lead to reduced voltage requirements in a system and feature stronger dependence of the output current on the electric field, as compared to traditional metals. At the same time, the early ignition and initially stronger current-electric field dependence of nonmetallic field emitters in low current regime (be it conventional silicon or carbon nanotube, CNT, fibers) gives way to current saturation when the emitter strongly departs from the Fowler-Nordheim (FN) law [19–28]. The existence of current satu-

ration effect was known for many decades and remains an outstanding, unsolved problem. The effect impacts the total output current and therefore remains a serious challenge and obstacle by impeding further improvement of current field emission device technologies and developments toward novel applications.

The current saturation cannot be explained by common space charge effect [29], because if experimentally determined onset saturation current is normalized by the formal emission area derived from the tip radius of a post/wire/needle like emitter, the current density remains orders of magnitude lower compared to the current density of  $\gtrsim 10^6$  A/cm<sup>2</sup>. The current density of  $\gtrsim 10^6$  A/cm<sup>2</sup> has been proved to promote the space charge effect that forces metal field emitters to deviate from the FN law [30]. Therefore, the saturation behavior is a general phenomenon specific to nonmetallic field emitters that have an explanation apart from the space charge effect. Other main mechanisms that are likely behind the current saturation effect are (1) surface termination of the emitting tip by foreign molecules that change the structure of the potential barrier for electrons to tunnel through [21]; applied voltage loss (2) along the field emitter or (3) at the interface between the emitter and its supporting bulk substrate/base that can be effectively described by the serial resistor model [31]. One of the main problems with the surface termination mechanism is that, on one hand, it lowers the turn-on field while, contradictory, it limits the output cur-

---

\* s.s.baturin@gmail.com

† serbar@msu.edu

rent. Also, molecular adsorbates do not seem to be causing current saturation in metallic emitters. Minoux et al., using simulations and experimental evidence for single CNT [24], and most recently Forbes, theoretically [32] demonstrated in elegant ways that the voltage loss, in other words significant resistance, along the field emitter post/wire should play a most significant role in the onset of the field emission current saturation. In Ref.[24], high temperature annealing experiments demonstrated that the improved emitting tip and the entire CNT crystallinity has enhanced the output current such that the saturation onset increased by three orders of magnitude. The presented facts suggest the importance of intrinsic factors (bulk material properties) over extrinsic factors (surface termination and space charge) behind the current saturation and FN law breakdown.

Here, taking the course of considering the mechanism of applied voltage loss along the field emitter due to bulk material properties, we propose a unified concept that explains the basic saturation mechanism, i.e. the nature of the hypothetical serial resistor, and the fundamental difference in the saturation behavior of nonmetallic materials. First, we derive the basic formula. Then, using the formula, we calculate all the current-voltage characteristics and compare against experimental curves for single-tip and arrayed *p*- and *n*-type Si emitters, and for single CNT and CNT fiber emitters. The proposed formalism could become a predictive tool to search for new prospective materials or to optimize existing ones, and could therefore solve the technological aspect of nonmetallic field emitter devices by helping boost their performance.

### Theoretical model

First we consider a nonmetallic layer and consider electron transport from the substrate to the nonmetal-vacuum boundary. By resolving and calculating the emission area, we know that emission is limited to a number of discrete emitting areas across the surface [28]. So we propose the conductive cylindrical channel concept as illustrated in Fig.1. Current that is flowing through the channel we express using well known formula

$$I_s = \frac{|e|N}{\Delta t}. \quad (1)$$

Here  $N$  is the number of electrons in the infinitely thin disk of an area  $\delta S$ ,  $e$  is the electron charge and  $\Delta t$  is the time of flight, i.e. time it takes an electron to travel from the substrate to the surface of the nonmetallic layer. If we assume that material is isotropic then the number of electrons  $N$  can be expressed through the electron volume density  $n$  as

$$N = n^2/3 \delta S. \quad (2)$$

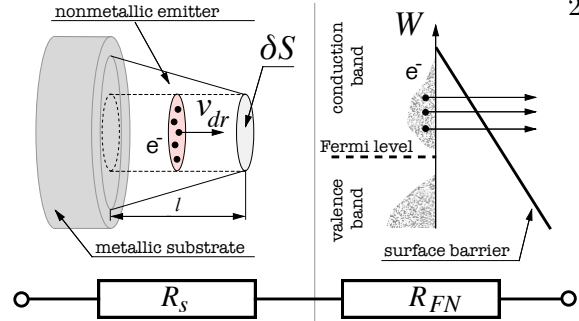


Figure 1: A schematic diagram of the proposed cylindrical channel electron transport and electron field emission.

Consequently, the current density can be written in the form

$$j_s = \frac{|e|n^{2/3}}{\Delta t}. \quad (3)$$

Time of flight  $\Delta t$  can be expressed through the drift velocity of electrons as

$$\Delta t = \frac{l}{v_{dr}(E)}. \quad (4)$$

Here  $l$  is the length of the conducting channel.

It is known [33] that drift velocity  $v_{dr}$  in a semiconductor and semiconductor devices [34] depends on the electric field  $E$  inside the bulk as

$$v_{dr}(E_b) = \frac{v_\infty \mu E_b}{(v_\infty^\gamma + \mu^\gamma E_b^\gamma)^{1/\gamma}}, \quad (5)$$

here  $v_\infty$  is the saturation drift velocity at high internal electric field,  $\mu$  is the charge carrier mobility and  $\gamma$  determines how sharply the drift velocity approaches the saturation velocity. It was found that  $\gamma$  is equal to 2 and 1 for electrons and holes, respectively. The saturation velocity  $v_\infty$  can be calculated through the free electron mass  $m_e$  and optical phonon energy  $W_{op}$  in traditional semiconductors as  $v_\infty = \sqrt{\frac{8W_{op}}{3\pi m_e}}$  and it is always very close to  $10^7$  cm/s. Typically, the saturation velocity is an experimentally determined quantity to be used together with formula (5). Moreover, regardless what scattering mechanisms are, even exceptionally high mobility ( $\sim 10^4$  cm<sup>2</sup>/(V.s) materials such as CNT [35] and graphene [36] and devices such as 2D electron gas HEMTs [37] also have saturation velocities close to  $10^7$  cm/s. We assume that if we apply external field  $E$  to the surface then internal field inside the bulk is simply  $E_b = E/\epsilon$ , where  $\epsilon$  is the relative dielectric permittivity. With this approximation we rewrite (5) as

$$v_{dr}(E) = \frac{v_\infty \mu E}{(\epsilon^\gamma v_\infty^\gamma + \mu^\gamma E^\gamma)^{1/\gamma}}. \quad (6)$$

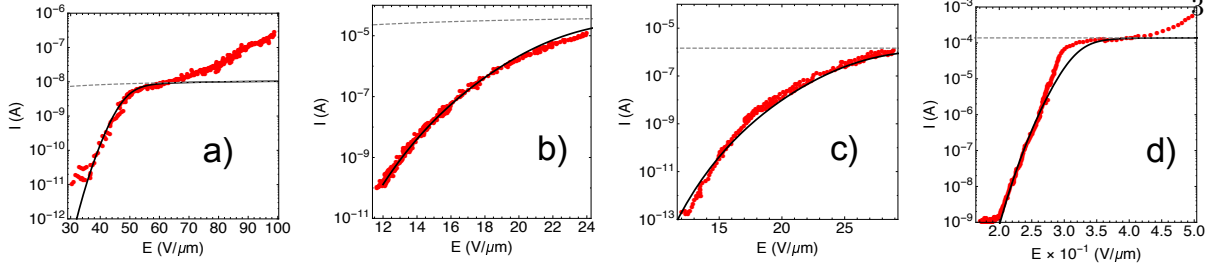


Figure 2: Comparison with the experimental results. Red dots are: a) Ref.[38] single  $p$ -type Si nano-tip, b) Ref.[39] array of  $n$ -type Si nano-tips, c) Ref.[24] single CNT d) Ref. [22] CNT fiber. Solid lines are formula (14) with corresponding parameters from Table I. Dashed lines are formula (7) with parameters from Table I with  $j_s(E)$  multiplied by  $S_{av}$ .

By combining (3), (4) and (6) we arrive at

$$j_s(E) = \frac{|e|n^{2/3}}{l} \frac{v_\infty \mu E}{(\varepsilon \gamma v_\infty^2 + \mu \gamma E \gamma)^{1/\gamma}}. \quad (7)$$

Formula (7) gives estimate of the maximum current density one can drain from a nonmetallic emitter under external field. Ultimately in the limit of a very high external field  $E \gg \varepsilon v_\infty / \mu$  we have

$$j_s^{\max} = \frac{|e|n^{2/3}v_\infty}{l}. \quad (8)$$

Next we consider electron field emission from the surface of the nonmetallic emitter to the vacuum. Field emission current density is usually approximated by FN law [30] as

$$j_{\text{FN}}(E) = a \frac{\beta^2 E^2}{\phi} \exp\left(-\frac{b\phi^{3/2}}{\beta E}\right). \quad (9)$$

Here  $E$  is the electric field on the surface,  $\beta$  is the field enhancement factor,  $\phi$  is the surface potential barrier height, and  $a = 1.54 \times 10^{-6}$  (A eV  $V^{-2}$ ) and  $b = 6.83$  (eV $^{-3/2}$  V nm $^{-1}$ ) are the FN constants.

We now consider an equivalent serial resistor model of the cylindrical channel as it is depicted in Fig.1. Total current that goes through nonmetal bulk and the potential barrier on the surface connected in series can be expressed in the terms of Ohm's law as

$$\delta I = \frac{U}{R_s + R_{\text{FN}}}. \quad (10)$$

Here  $U$  is an external voltage and  $R_s$  is the equivalent resistance of the bulk and  $R_{\text{FN}}$  is the equivalent resistance of the FN process. Now, if we assume that electric field screening by the field emission electron current is low, the field on the nonmetal surface will be approximately independent of the emission (FN) current. On the other

hand, that means that voltage across the emitter will be approximately  $U \approx El$ . The resistance of the emitter and the equivalent FN resistance can then be expressed through the corresponding current densities as

$$R_s(E) = \frac{El}{j_s(E)\delta S}, \quad (11)$$

$$R_{\text{FN}}(E) = \frac{El}{j_{\text{FN}}(E)\delta S}. \quad (12)$$

We note, the formulas (10) and (11) are constructed such that they guarantee exact currents  $I_s = j_s \delta S$  and  $I_{\text{FN}} = j_{\text{FN}} \delta S$  in two limiting cases when  $R_s \gg R_{\text{FN}}$  and  $R_s \ll R_{\text{FN}}$ , respectively. With (10) we have for the total current

$$\delta I(E) = \frac{j_s(E)j_{\text{FN}}(E)}{j_s(E) + j_{\text{FN}}(E)} \delta S. \quad (13)$$

Taking into account that the emission area is an electric field dependent property [28], we can write the total emission current measured in experiment as

$$I(E) = \frac{j_s(E)j_{\text{FN}}(E)}{j_s(E) + j_{\text{FN}}(E)} S(E), \quad (14)$$

here  $S(E)$  is the emission area,  $j_s(E)$  is given by (7) and  $j_{\text{FN}}(E)$  is given by (9).

We test the proposed model against four representative experimental result sets [22, 24, 38, 39]. It is clear from the comparison on Fig.2, our model remarkably predicts the onset kink point when experimental data start deviating from the FN law, as well as it quantitatively predicts the saturation current plateau  $I_s^{\max} = \frac{|e|n^{2/3}v_\infty}{l} \delta S$ , i.e. the total current to be taken away from the nonmetallic field emitter cannot exceed this value. In addition to that, there are few more consequences of our analysis:

(1) During photon-assisted field emission experiments the output current always goes up because

Table I: Parameters for the crosscheck with the experimental data

type	number of emitters	$\phi$ (eV)	$\mu$ (cm <sup>2</sup> /V·s)	$n$ (cm <sup>-3</sup> )	$\varepsilon$	$v_\infty$ (cm/s)	$S_{av}$ (cm <sup>2</sup> )	$l$ (cm)	$\beta$
<i>p</i> -type Si	1 [38]	4.7	450 [40]	$3 \times 10^{15}$	12	$8 \times 10^6$ [40]	$\sim 2.82 \times 10^{-11}$ [38]	$6 \times 10^{-5}$ [38]	95
<i>n</i> -type Si	$\sim 100$ [39]	4.7	100 [40]	$5 \times 10^{19}$	12	$10^7$ [40]	$\sim 1.26 \times 10^{-9}$ [39]	$5.7 \times 10^{-4}$ [39]	265
CNT	1 [24]	5.0	2,000	$\sim 3 \times 10^{19}$	1	$10^7$ [35]	$\sim 2.82 \times 10^{-11}$ [24]	$3 \times 10^{-4}$ [24]	260
CNT fiber	1 [22]	5.0	10,000 [41, 42]	$\sim 1.5 \times 10^{19}$	10	$10^7$ [35]	$\sim 7.07 \times 10^{-6}$ [22]	0.5 [22]	13,500

the supply term  $N$  increases (increased electron supply generated by light).

(2) During heat-assisted field emission experiments the output current always goes up because of the additional thermionic emission mechanism (current is indeed linear in Richardson coordinates [43, 44]). As the current saturation plateau grows higher with temperature increasing, it is predicted to flatten more. The mobility and the saturation velocity are responsible for this flattening effect because  $\mu$  and  $v_\infty$  both steadily diminish at temperatures in excess of the room temperature.

(3) With all other parameters fixed, the emission surface area can be calculated.

#### *Cross check with the experiment*

As far as no data on  $S(E)$  dependence was available we picked two experiments that were performed on individual emitters, as we were able to accurately estimate the emission area by using electron micrograph images of those emitter tips [22, 24, 38]. In the experiment with arrayed *n*-type Si emitters [39], the total emission area was estimated by taking the number of emitters into account. In the experiment with a macroscopic CNT fiber emitter [22], the total emission area was estimated by using the radius of the fiber reported by the authors. Estimated emission area values  $S_{av}$  along with all other parameters used in calculations are listed in Table I. Other parameters like drift velocity and carrier mobility were taken from the online data base of the Ioffe institute [40].

All experimental data was extracted by digitizing figures of current-voltage curves in the corresponding reference [22, 24, 38, 39].

When plotting theoretical curve all parameters in the final equation were fixed except  $\beta$  and  $S_{av}$  that were varied slightly to achieve the best fit. We note that obtained fitting  $\beta$ -factor values were

in close match with  $\beta$ -factors or aspect ratio values reported by the authors of the experiments used for model cross check comparison.

#### *Conclusion*

It was shown that the phenomenon of current saturation in nonmetallic field emitters, in a way that they stop obeying the Fowler-Nordheim law, has a clear physical reason. Namely, the output current is saturated/limited by the maximal number of electrons could be delivered to the emission point on the surface through the emitter bulk in the direction perpendicular to the surface, i.e. it is a combination of how many electrons are available, how fast and how far they have to travel, how many exit channels on the surface are available at a given external electric field. Using the simplified and commonly considered serial resistor model and the fundamental regularities of charge carrier transport in semiconductors, a unified concept and mathematical formalism that quantitatively describes the current saturation phenomenon was proposed. The model demonstrates excellent agreement with available experimental data and could be used as a predictive tool to search of new prospective field emitter materials.

#### **ACKNOWLEDGMENTS**

SSB was supported by the U.S. National Science Foundation under Award No. PHY-1549132, the Center for Bright Beams, and under Award No. PHY-1535639. AVZ was supported by the U.S. Department of Energy, Office of Science, Materials Sciences and Engineering Division. S.V.B. was supported by funding from the College of Engineering, Michigan State University, under Global Impact Initiative.

- 
- [1] Y. Kohno, E. Okunishi, T. Tomita, I. Ishikawa, T. Kaneyama, Y. Ohkura, Y. Kondo, and T. Isabell, *Microscopy Anal.* **24**, S9 (2010).  
[2] S. Tsujino, P. Das Kanungo, M. Monshipouri, C. Lee, and R. J. D. Miller,

- Nature Commun.* **7**, 13976 (2016).  
[3] S. Cheng, F. A. Hill, E. V. Heubel, and L. F. Velásquez-García, *J. Microelectromechanical Systems* **24**, 373 (2015).  
[4] E. J. Radauscher, A. D. Keil, M. Wells, J. J. Ams-

- den, J. R. Piascik, C. B. Parker, B. R. Stoner, and J. T. Glass, *J. Am. Soc. Mass Spec.* **26**, 1903 (2015).
- [5] D. Temple, *Mater. Sci. Engineering R* **24**, 185 (1999).
- [6] D. R. Whaley, R. Duggal, C. M. Armstrong, C. L. Bellew, C. E. Holland, and C. A. Spindt, *IEEE Trans. Electron Devices* **56**, 896 (2009).
- [7] M. Garven, S. N. Spark, A. W. Cross, S. J. Cooke, and A. D. R. Phelps, *Phys. Rev. Lett.* **77**, 2320 (1996).
- [8] C. Brau, *Nucl. Instrum. Methods Phys. Res. A* **407**, 1 (1998).
- [9] S. V. Baryshev, S. Antipov, J. Shao, C. Jing, K. J. P. Quintero, J. Qiu, W. Liu, W. Gai, A. D. Kanareykin, and A. V. Sumant, *Appl. Phys. Lett.* **105**, 203505 (2014).
- [10] D. Bock, P. Laufer, and M. Tajmar, in *2017 30th International Vacuum Nanoelectronics Conference (IVNC)* (IEEE, 2017) pp. 96–97.
- [11] C. A. Spindt, *J. Appl. Phys.* **39**, 3504 (1968).
- [12] C. A. Spindt, I. Brodie, L. Humphrey, and E. R. Westerberg, *J. Appl. Phys.* **47**, 5248 (1976).
- [13] W. Choi, I. Lahiri, R. See-laboyina, and Y. S. Kang, *Critical Rev. Solid State Mater. Sci.* **35**, 52 (2010).
- [14] M. L. Terranova, S. Orlanducci, M. Rossi, and E. Tamburri, *Nanoscale* **7**, 5094 (2015).
- [15] H. Yamaguchi, K. Murakami, G. Eda, T. Fujita, P. Guan, W. Wang, C. Gong, J. Boisse, S. Miller, M. Acik, K. Cho, Y. J. Chabal, M. Chen, F. Wakaya, M. Takai, and M. Chhowalla, *ACS Nano* **5**, 4945 (2011).
- [16] B. R. Stoner and J. T. Glass, *Nature Nanotech.* **7**, 485 (2012).
- [17] E. J. Radauscher, K. H. Gilchrist, S. T. D. Dona, Z. E. Russell, J. R. Piascik, J. J. Amsden, C. B. Parker, B. R. Stoner, and J. T. Glass, *IEEE Trans. Electron Devices* **63**, 3753 (2016).
- [18] C. Li, M. T. Cole, W. Lei, K. Qu, K. Ying, Y. Zhang, A. R. Robertson, J. H. Warner, S. Ding, X. Zhang, B. Wang, and W. I. Milne, *Adv. Functional Mater.* **24**, 1218 (2014).
- [19] R. L. Perry, *J. Appl. Phys.* **33**, 1875 (1962).
- [20] P. G. Collins and A. Zettl, *Appl. Phys. Lett.* **69**, 1969 (1996).
- [21] K. A. Dean and B. R. Chalamala, *Appl. Phys. Lett.* **76**, 375 (2000).
- [22] M. Cahay, P. T. Murray, T. C. Back, S. Fairchild, J. Boeckl, J. Bulmer, K. K. K. Koziol, G. Gruen, M. Sparkes, F. Orozco, and W. O’Neill, *Appl. Phys. Lett.* **105**, 173107 (2014).
- [23] P. Serbun, *A systematic investigation of carbon, metallic and semiconductor nanostructures for field-emission cathode applications*, Ph.D. thesis, University of Wuppertal (2014).
- [24] E. Minoux, O. Groening, K. B. K. Teo, S. H. Dalal, L. Gangloff, J.-P. Schnell, L. Hudanski, I. Y. Y. Bu, P. Vincent, P. Legagneux, G. A. J. Amaratunga, and W. I. Milne, *Nano Lett.* **5**, 2135 (2005).
- [25] J. Robertson, *J. Vac. Sci. Technol. B* **17**, 659 (1999).
- [26] C. Ducati, E. Barborini, P. Piseri, P. Milani, and J. Robertson, *J. Appl. Phys.* **92**, 5482 (2002).
- [27] D. Varshney, C. V. Rao, M. J.-F. Guinel, Y. Ishikawa, B. R. Weiner, and G. Morell, *J. Appl. Phys.* **110**, 044324 (2011).
- [28] O. Chubenko, S. S. Baturin, K. K. Kovi, V. Sumant, and S. V. Baryshev, *ACS Appl. Mater. Interfaces* **9**, 33229 (2017).
- [29] J. P. Barbour, W. W. Dolan, J. K. Trolan, E. E. Martin, and W. P. Dyke, *Phys. Rev.* **92**, 45 (1953).
- [30] R. H. Fowler and L. Nordheim, *Proc. Royal Soc. A* **119**, 173 (1928).
- [31] M. Bachmann, F. Dams, F. Düsberg, M. Hofmann, A. Pahlke, C. Langer, R. Lawrowski, C. Prommesberger, R. Schreiner, P. Serbun, D. Lützenkirchen-Hecht, and G. Müller, *J. Vac. Sci. Technol. B* **35**, 02C103 (2017).
- [32] R. G. Forbes, *Appl. Phys. Lett.* **110**, 133109 (2017).
- [33] S. M. Sze and K. K. Ng, *Physics of Semiconductor Devices (3rd edition)* (Wiley, 2007).
- [34] D. Greenberg and J. del Alamo, *IEEE Trans. Electron Devices* **41**, 1334 (1994).
- [35] Y.-F. Chen and M. S. Fuhrer, *Phys. Rev. Lett.* **95**, 236803 (2005).
- [36] I. Meric, M. Han, A. Young, B. Ozyilmaz, P. Kim, and K. Shepard, *Nature Nanotech.* **3**, 654 (2008).
- [37] J. del Alamo, *Nature* **479**, 317 (2011).
- [38] P. Serbun, B. Bornmann, A. Navitski, G. Müller, C. Prommesberger, C. Langer, F. Dams, and R. Schreiner, *J. Vac. Sci. Technol. B* **31**, 02B101 (2013).
- [39] C. Langer, R. Lawrowski, C. Prommesberger, F. Dams, P. Serbun, M. Bachmann, G. Müller, and R. Schreiner, in *Vacuum Nanoelectronics Conference (IVNC), 2014 27th International* (IEEE, 2014) p. doi: 10.1109/IVNC.2014.6894824.
- [40] “Ioffe institute materials data base,” (2017).
- [41] Y.-L. Li, I. A. Kinloch, and A. H. Windle, *Science* **304**, 276 (2004).
- [42] A. Lekawa-Raus, J. Patmore, L. Kurzepa, J. Bulmer, and K. Koziol, *Adv. Funct. Mater.* **24**, 3661 (2014).
- [43] M. Choueib, R. Martel, C. S. Cojocar, A. Ayari, P. Vincent, and S. T. Purcell, *ACS Nano* **6**, 7463 (2012).
- [44] S. Mingels, V. Porshyn, C. Prommesberger, C. Langer, R. Schreiner, D. Lützenkirchen-Hecht, and G. Müller, *J. Appl. Phys.* **119**, 165104 (2016).